

Supporting Material

Skin membrane electrical impedance properties under the influence of a varying water gradient

Sebastian Björklund, Tautgirdas Ruzgas, Agnieszka Nowacka, Ihab Dahi, Daniel Topgaard, Emma Sparr, Johan Engblom

Supporting Text

A. Alternative equivalent circuit

Other equivalent circuits were considered for analysis of the impedance data, consisting of parallel combinations of resistors and capacitors, with or without a CPE element (1, 2). However, equivalent circuits based on ideal elements did not reflect our impedance data adequately and is therefore not considered further. The circuit in Fig. S2 was used to evaluate our impedance data to allow for a comparison with the results obtained with the circuit in Fig. S1 B. This analysis is summarized in Table S1 and S2 for membranes A and B, respectively. By analyzing the change of the parameters in these tables we get following changes in average: R_0 and R_1 are 15 and 11 times higher for the less hydrated skin membrane, respectively. C_1 is 1.2 higher for the fully hydrated skin membrane. These trends are in agreement with the corresponding values of R_{mem} and C_{eff} presented in the main article where R_{mem} was in average 15 times higher for the less hydrated skin membrane and C_{eff} was 1.5 higher for the fully hydrated skin membrane. We note that the relative change of C_1 is slightly lower as compared to C_{eff} , but this does not change the main conclusions in our article. In conclusion, it is clear that the general trends is consistent with the observed trends in our work where the circuit in Fig. S1 B was employed. However, we are not fully convinced of the physical connection of the elements in the circuit in Fig. S2 to the SC structure. There is no clear evidence supporting that e.g. R_0 and R_1 can be connected to specific regions inside SC, such as the intracellular domains of the corneocytes or extracellular lipid lamellar structures. This dilemma, regarding the uncertain connection of the elements to the SC structure, is less manifested by the circuit in Fig. S1 B as it does not discriminate between different, and less certain, current pathways and capacitive regions. Based on this analysis we must conclude that including an extra RC circuit only adds more discussion without proving or disproving undoubtedly any point.

B. Determination of solution resistance (R_{sol}) and membrane resistance (R_{mem})

Fig. S3 shows impedance data of a skin membrane with a water gradient varying over time. The data are presented as impedance plane plots with frequency as a parameter (the frequency decreases along the x-axis). All impedance data on skin membranes displayed the same characteristic pattern of a depressed semi-circle. The impedance data approaches the real axis at high frequencies (left side) and low frequencies (right side), where Z_{Im} approaches zero. At high frequencies Z_{Re} represents R_{sol} and at low frequencies $Z_{\text{Re}} = R_{\text{sol}} + R_{\text{mem}}$. R_{sol} and R_{mem} were determined by fitting the data in impedance plane plots to the equivalent circuit (Fig. S1 B) using Ivium software. All data were normalized with the skin membrane area (0.64 cm^2) to get units in Ohm cm^2 . The fitted data of R_{sol} , for PBS and PEG solutions, were

in agreement with the solution resistance without any skin membrane present. The PBS and PEG solutions were purely resistive over the impedance frequency range (i.e. zero phase difference between voltage and current). R_{sol} was about 200 Ohm when both the receptor and donor chambers of the Franz cell were filled with PBS ($a_{w,d}=0.992$) and about 1500 Ohm when 65 wt % PEG solution was used as donor solution ($a_{w,d}=0.826$). However, it should be noted that the measured value of R_{sol} depends on the precise distance between the reference and sensing electrodes, which in the present experiments was subject to small variations. Therefore small deviations from the separately determined values of the solution resistance were expected and accepted. R_{sol} was in all cases at least an orders of magnitude lower than R_{mem} . Thus, the effect of the uncertainty of R_{sol} on the determined value of R_{mem} is negligible. Fig. S3 shows that there is a clear difference in R_{mem} as the water gradient is changed. After 24 h with $a_{w,d}=0.826$ the semi-circles approaches the real axis at low frequency at significantly higher values compared to the case of $a_{w,d}=0.992$. The impedance data corresponding to the case when $a_{w,d}=0.992$ are presented in close up in Fig. S3 B. A compilation of the impedance data, corresponding to the measurements in Fig. S3, is presented in Table S3. The values of the CPE parameters (α and Q_{eff}) and C_{eff} were calculated according to the method described in the main article.

Several publications report on the effect of perturbing current densities, e.g. (3-5), where in all cases a continuous decrease in the total impedance was observed for each scan that followed an applied perturbing current. This was not observed in the present work suggesting that the impedance measurements performed here were noninvasive regarding to the skin barrier integrity.

C. Justification of usage of SC samples in NMR and x-ray measurements and excised skin membranes in impedance experiments

The electrical impedance of skin resides mainly within the SC, while the underlying layers have orders of magnitude lower impedance (6-8). In other words, the observed changes of the skin membrane electrical properties of are mainly attributed to effects occurring in the SC. This justifies the employment of SC samples in the solid-state NMR and x-ray diffraction experiments. Further, at steady state conditions, the outermost parts of SC is in local equilibrium with the water activity of the contacting solution. This rationalize the comparison between the impedance measurements (where a gradient in water activity is present across the skin membrane) and the NMR and x-ray experiments (where the SC sample is in equilibrium with the surrounding solution, i.e. no gradient).

D. The effect of R_{sol} on R_{mem}

We note that R_{mem} can be affected by the solution resistance (5, 9), which in the present work varied between $R_{sol} \sim 1500$ Ohm (65 wt% PEG in PBS solution) and $R_{sol} \sim 200$ Ohm (neat PBS solution). Two control experiments were performed to investigate this possibility. The first experiment was performed on inert membranes (Cellulose ester dialysis membranes, Spectra/Por®Biotech, MWCO 500 Da, Spectrum Laboratories). The results are presented in Fig. S7 and show about a threefold increase in R_{mem} in the case of higher R_{sol} . The second experiment was performed in a similar manner as the experiments described in the present study (i.e. 96 h experiment on skin membrane). However, instead of applying the PEG solution, the solution resistance was adjusted to about 1500 Ohm (PBS solution with 10 mM

NaCl). The results showed that R_{mem} was less than 4 times higher in average when R_{sol} was 1500 Ohm compared to when R_{sol} was 200 Ohm (see Table S4). In addition, the consecutive values of C_{eff} from this experiment were 22.2 nF cm⁻² (24 h), 29.5 nF cm⁻² (48 h), 39.7 nF cm⁻² (72 h) and 37.7 nF cm⁻² (96 h). This gradual increase of C_{eff} differs from the observed switch-behavior between lower and higher values of C_{eff} in the case of a varying water gradient. Taken together, these control experiments show that the mechanisms responsible for the changes in the electrical properties of the skin membrane, as a consequence of a varying water gradient, cannot simply be explained by the variations of R_{sol} .

Supporting Figures

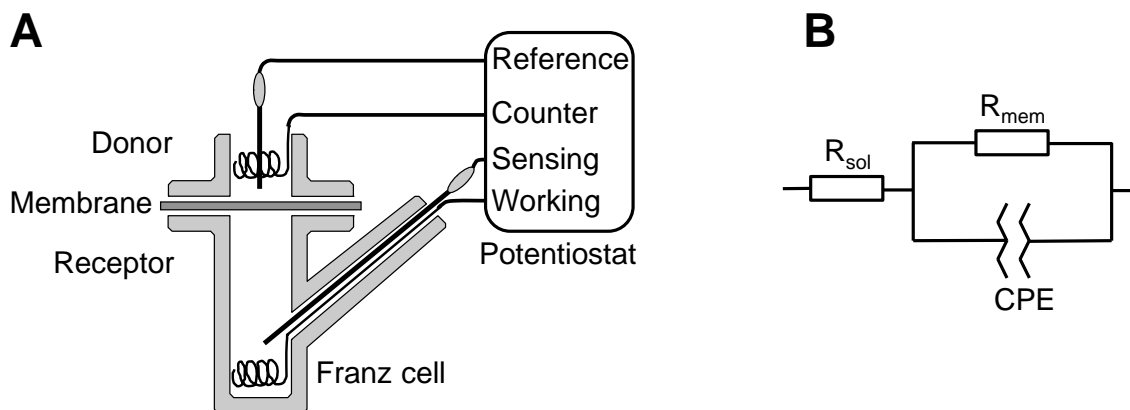


FIGURE S1. (A) Schematic representation of the Franz cell ($\varnothing=0.90$ cm, $V=6$ ml, PermeGear, Hellertown, PA, USA) equipped with four electrodes for electrical impedance measurements. Two platinum wires served as working and counter electrodes and two Ag/AgCl/3M KCl electrodes from World Precision Instruments (Sarasota, FL, USA) were used as sensing and reference electrodes. The water jacket of the Franz cell was kept at 32 °C by a circulating water bath. (B) Equivalent electrical circuit used to model the experimental impedance data. R_{sol} is the resistance of the donor and receptor solution, R_{mem} is the membrane resistance, and CPE is a constant-phase element.

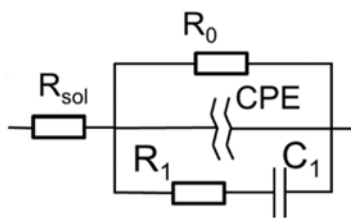


FIGURE S2. An alternative equivalent circuit used to evaluate the impedance data. The results from this analysis is compiled in Table S1 and S2 for membrane A and B, respectively.

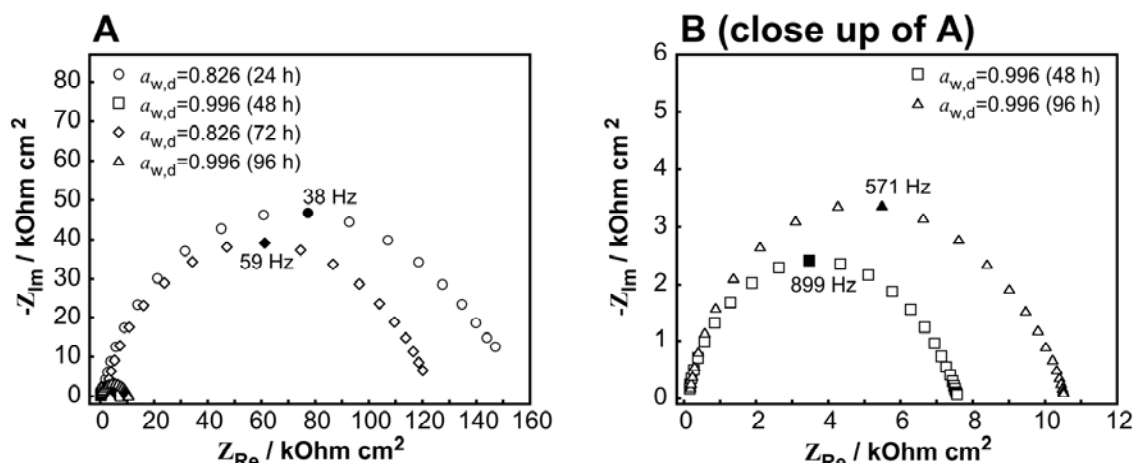


FIGURE S3. (A) Impedance plane plots of experimental data for skin membrane at different hydrating conditions. The external water gradient is defined by the water activity of the donor ($a_{w,d}$) and receptor ($a_{w,r}$) solutions. The water activity of the receptor solution was constant at $a_{w,r}=0.992$. The characteristic frequency where the imaginary part of the impedance has its maximum is indicated for each impedance scan. (B) Close up of (A) with the data from $a_{w,d}=0.992$.

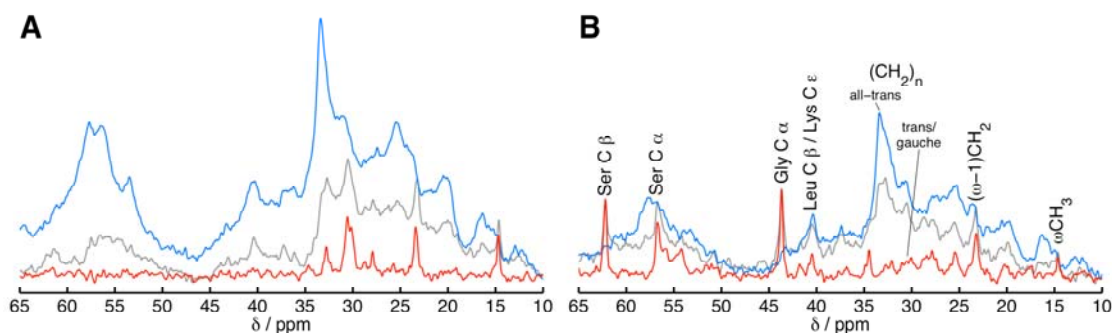


FIGURE S4. Molecular dynamics of SC components using DP (grey), CP (blue), and INEPT (red) pulse sequences for signal enhancement of molecular segments in either rigid (CP) or mobile (INEPT) microenvironments. ^{13}C spectra of pulverized SC equilibrated at (A) 80% RH and (B) 99.5% RH. Resonance lines from keratin filament amino acid residues and lipids are labeled in (B). The intensity is scaled to give equal DP signal of the peak centered around 32.8 ppm due to different amounts of SC sample in each experiment.

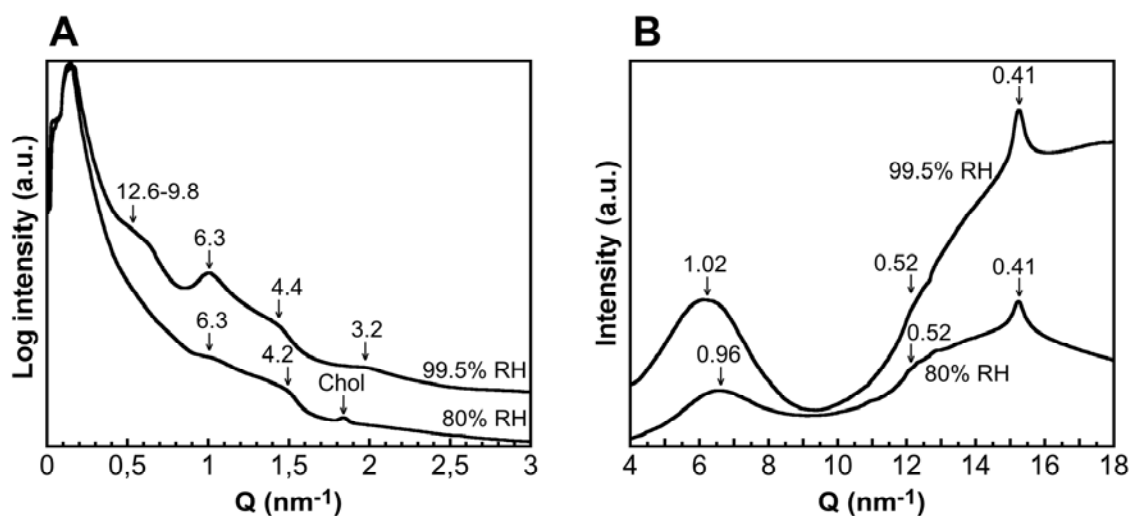


FIGURE S5. SAXS (A) and WAXS (B) data on pulverized SC equilibrated at 80% RH and 99.5% RH. Numbers associated with an arrow give the d -spacing (nm). Chol is crystalline cholesterol.

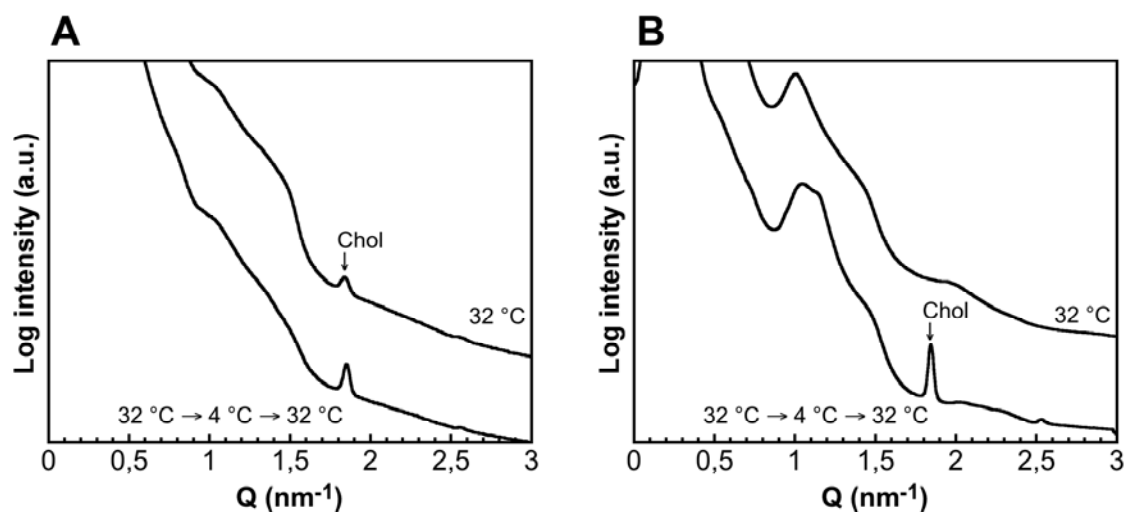


FIGURE S6. SAXS data on pulverized SC samples equilibrated at (A) 80% RH and (B) 99.5% RH illustrating that the sample preparation may affect the occurrence of phase separated crystalline cholesterol (chol). Top curves are the same as in Fig. S5, while the bottom curves are from SC samples equilibrated at 32 °C, loaded into the sample cell, cooled to 4 °C for approx. 12 h, and finally measured at 32 °C. The samples exposed to low temperature are associated with more intense peaks from phase separated crystalline cholesterol.

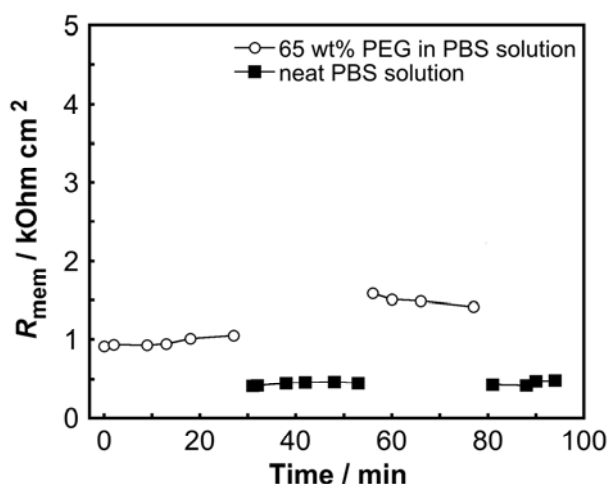


FIGURE S7. Membrane resistance (R_{mem}) of dialysis membrane (cutoff 500 Da) when in contact with 65 wt% PEG in PBS solution or neat PBS solution. In average the membrane resistance was less than 3 times higher in the case of PEG solution.

Supporting Tables

TABLE S1. Impedance circuit parameters for membrane A evaluated with the circuit in Fig. S2.

Time / h	$a_{w,d}$	$R_0 /$ kOhm cm^2	$R_1 /$ kOhm cm^2	$C_1 /$ nF cm^{-2}	α	$Q /$ $\text{Ohm}^{-1} \text{cm}^{-2} \text{s}^\alpha$
24 h	0.826	144.6	1564.8	20.9	0.771	6.40×10^{-8}
48 h	0.992	7.4	101.3	15.5	0.784	20.6×10^{-8}
72 h	0.826	121.6	2241.3	10.3	0.763	4.98×10^{-8}
96 h	0.992	10.4	117.1	18.3	0.798	20.4×10^{-8}

TABLE S2. Impedance circuit parameters for membrane B evaluated with the circuit in Fig. S2.

Time / h	$a_{w,d}$	$R_0 /$ kOhm cm^2	$R_1 /$ kOhm cm^2	$C_1 /$ nF cm^{-2}	α	$Q /$ $\text{Ohm}^{-1} \text{cm}^{-2} \text{s}^\alpha$
24 h	0.826	115.8	1329	12.5	0.826	19.8×10^{-8}
48 h	0.992	5.8	122	15.4	0.831	48.8×10^{-8}
72 h	0.826	44.2	851	12.7	0.837	26.8×10^{-8}
96 h	0.992	5.6	187	16.6	0.836	52.9×10^{-8}

TABLE S3. Impedance circuit parameters from the data in Fig. S3 (cf. Fig. 2 A and B in the main article).

Time / h	$a_{w,d}$	$R_{\text{mem}} /$ kOhm cm^2	α	$Q_{\text{eff}} /$ $\text{Ohm}^{-1} \text{cm}^{-2} \text{s}^\alpha$	$C_{\text{eff}} /$ nF cm^{-2}
24 h	0.826	149.5	0.809	6.89×10^{-8}	23.4
48 h	0.992	7.4	0.769	21.4×10^{-8}	31.0
72 h	0.826	120.7	0.789	8.01×10^{-8}	23.1
96 h	0.992	10.5	0.788	15.5×10^{-8}	27.4

Table S4. Impedance circuit parameters parameters for a skin membrane in contact with PBS solution with 10 mM NaCl (24 h and 72 h) or 131 mM NaCl (48 h and 96 h).

Time / h	R_{sol} / Ohm	R_{mem} / kOhm cm^2	α	Q_{eff} / Ohm $^{-1}$ cm^{-2} s^{α}	C_{eff} / nF cm^{-2}
24 h	1500	36.8	0.850	6.5×10^{-8}	22.3
48 h	200	9.0	0.793	16×10^{-8}	29.5
72 h	1500	12.2	0.733	30×10^{-8}	39.7
96 h	200	4.9	0.751	32×10^{-8}	37.7

Supporting References

1. Kontturi, K., and L. Murto. 1994. Impedance spectroscopy in human skin. A refined model. *Pharm. Res.* 11:1355-1357.
2. Pliquett, F., and U. Pliquett. 1996. Passive electrical properties of human stratum corneum in vitro depending on time after separation. *Biophysical Chemistry* 58:205-210.
3. Foley, D., J. Corish, and O. I. Corrigan. 1992. Iontophoretic delivery of drugs through membranes including human stratum corneum. *Solid State Ionics* 53-56:184-196.
4. Membrino, M. A. 2002. Transdermal delivery of therapeutic compounds by iontophoresis. Ph.D. Thesis, Chemical Engineering, University of Florida, Gainesville, Florida.
5. Oh, S. Y., L. Leung, D. Bommannan, R. H. Guy, and R. O. Potts. 1993. Effect of current, ionic strength and temperature on the electrical properties of skin. *J. Control. Release* 27:115-125.
6. Yamamoto, T., and Y. Yamamoto. 1976. Electrical properties of the epidermal stratum corneum. *Med. Biol. Eng.* 14:151-158.
7. Kalia, Y. N., F. Pirot, and R. H. Guy. 1996. Homogeneous transport in a heterogeneous membrane: water diffusion across human stratum corneum in vivo. *Biophys. J.* 71:2692-2700.
8. Clar, E. J., C. P. Her, and C. G. Sturrelle. 1975. Skin impedance and moisturization. *J. Soc. Cosmet. Chem.* 26:337-353.
9. DeNuzzio, J. D., and B. Berner. 1990. Electrochemical and iontophoretic studies of human skin. *J. Control. Release* 11:105-112.